Diabetologia (2012) 55:2835–2844
DOI 10.1007/s00125-012-2625-y

ARTICLE

Reduction of experimental diabetic vascular leakage and pericyte apoptosis in mice by delivery of αA-crystallin with a recombinant adenovirus

Y. H. Kim · S. Y. Park · J. Park · Y. S. Kim · E. M. Hwang · J. Y. Park · G. S. Roh · H. J. Kim · S. S. Kang · G. J. Cho · W. S. Choi

Received: 17 April 2012 / Accepted: 23 May 2012 / Published online: 8 July 2012

Abstract
Aims/hypothesis The study aimed to evaluate the efficacy of recombinant adenovirus expressing αA-crystallin (Ad-*αAc-Gfp*) in reducing pericyte loss within retinal vasculature in early diabetes.
Methods Diabetes was induced by streptozotocin injection into C57BL/6 mice. Ad-*αAc-Gfp* was delivered by intravitreous injection to the right eyes of mice 2 weeks before induction of diabetes. Vascular leakage was determined by fluorescent angiography, Evans Blue leakage assay and leucocyte adhesion test. Production of αA-crystallin was analysed by immunoblotting and double immunostaining and pericyte loss was analysed by pericyte count.
Results Vessel leakage and pericyte loss were observed in the streptozotocin-induced diabetic retina. Decreased abundance of αA-crystallin in retinas 2 and 6 months after the induction of diabetes was confirmed by two-dimensional electrophoretic analysis, immunoblotting and RT-PCR. Double immunofluorescence staining for αA-crystallin and NG2 chondroitin sulphate proteoglycan revealed that αA-crystallin was predominantly produced in the retinal pericyte and that the number of αA-crystallin-producing pericytes decreased in the diabetic retina. Retinal infection with Ad-*αAc-Gfp* led to decreased pericyte loss and vascular leakage compared with control.
Conclusions/interpretation Intravitreal delivery of Ad-*αAc-Gfp* protects against vascular leakage in the streptozotocin-induced model of diabetes. This effect is associated with the inhibition of diabetic retinal pericyte loss in early diabetes, suggesting that αA-crystallin has a role in preventing the pathogenesis of early diabetic retinopathy.

Keywords αA-Crystallin · BRB breakdown · Diabetic retinopathy · Pericyte loss

Y. H. Kim and S. Y. Park contributed equally to this study.

Electronic supplementary material The online version of this article (doi:10.1007/s00125-012-2625-y) contains peer-reviewed but unedited supplementary material, which is available to authorised users.

Y. H. Kim · S. Y. Park · J. Park · Y. S. Kim · G. S. Roh · H. J. Kim · S. S. Kang · G. J. Cho · W. S. Choi (✉)
Department of Anatomy and Neurobiology, Medical Research Center for Neural Dysfunction, Institute of Health Science, School of Medicine, Gyeongsang National University, 92 Chilam-dong, Jinju, Gyeongnam 660-751, Republic of Korea
e-mail: choiws@gnu.ac.kr

E. M. Hwang
Center for Functional Connectomics, Korea Institute of Science and Technology, Seoul, Republic of Korea

J. Y. Park
Department of Physiology, School of Medicine, Gyeongsang National University, Jinju, Republic of Korea

Abbreviations

Ad-*αAc-Gfp*	Recombinant adenovirus expressing αA-crystallin
BAX	BCL2-associated X protein
BCL2	B cell leukaemia/lymphoma 2
BRB	Blood–retinal barrier
2-DE	Two-dimensional electrophoresis
FITC-dextran	High-molecular-weight-FITC-conjugated dextran
GFP	Green fluorescent protein
HRP	Human retinal pericyte
MALDI-TOF	Matrix-assisted laser desorption ionisation time-of-flight
NG2	NG2 chondroitin sulphate proteoglycan
PARP	Poly-ADP-ribose-polymerase

PFA	Paraformaldehyde
PMF	Peptide mass fingerprinting
α-SMA	α-Smooth muscle actin
STZ	Streptozotocin
TEM	Transmission electron microscopy
TMR	Tetramethylrhodamine
TMR-dextran	TMR-conjugated dextran
TRITC	TMR-isothiocyanate
VEGF	Vascular endothelial growth factor

Introduction

Diabetic retinopathy is the major cause of blindness in diabetic patients and induces progressive damage to the retinal microvasculature [1]. Blood–retinal barrier (BRB) breakdown and consequent vessel leakage in the retina are the main events in the pathogenesis of diabetic retinopathy [2, 3]. Pericytes sheathing retinal capillary endothelial cells play a role in regulating endothelial cell proliferation and survival [4, 5]. Pericyte loss is considered a hallmark of diabetic retinopathy, and is associated with the development of vessel leakage and leucocyte adhesion, which signify BRB breakdown [6–8]. Pericyte loss is thought to occur via activation of key apoptotic proteins in the diabetic retina [9]. However, the underlying molecular mechanisms are currently unclear.

The α-crystallins are a family of small heat-shock proteins that perform many physiological functions, including the maintenance of cell survival [10, 11]. α-Crystallins not only possess chaperone-like activity in vitro, but also remodel and protect the cytoskeleton, inhibit apoptosis and enhance the resistance of cells to stress [12]. α-Crystallins can be either of two gene products: αA- and αB-crystallin. αA-Crystallin is predominantly produced in the lens and retina, while αB-crystallin is widely distributed in non-lenticular tissues [13]. A previous study reported that αA-crystallin is more protective against apoptosis than αB-crystallin in cultured lens epithelial cells [14]. Moreover, overproduction of αA- or αB-crystallin enhances resistance to thermal, photochemical and other stress conditions [10, 14]. Overproduction of αB-crystallin significantly reduces the apoptosis triggered by dicarbonyl-modified fibronectin in retinal capillary pericytes [15]. In view of the protective effects of α-crystallins in preserving the integrity of mitochondria, restricting the release of cytochrome *c*, blocking the degradation of poly-ADP-ribose-polymerase (PARP) and repressing the activation of caspase-3 [16], these proteins could be novel targets in gene-based therapy for early diabetic retinopathy.

The chaperone activity of αA-crystallin in the retina decreases significantly with ageing. The decreased production of αA-crystallin and increased truncation at the C- and N-terminals with ageing, together with its oxidation, suggest a general decrease in chaperone activity in the retina [17, 18]. Consistent with this, streptozotocin (STZ)-induced diabetic rats with uncontrolled hyperglycaemia show substantial loss of α-crystallin chaperone function [19, 20]. Diabetes strongly reduces the chaperone function of α-crystallins by reducing their solubility and disrupting the normal interaction of α-crystallins with BAX [21]. Studies using αA- and/or αB-crystallin-knockout mice have revealed increased retinal cell death in endophthalmitis and uveitis models, suggesting that α-crystallin prevents retinal cell death during inflammation [22, 23]. It is also reported that the absence of αB-crystallin leads to dramatic attenuation of angiogenesis via modulation of vascular endothelial growth factor (VEGF) in models of intraocular disease [24]. These functions have been implicated in disease process, and therefore α-crystallins may be effective targets for disease therapy. However, their physiological significance in the context of the pathological vasculature in diabetes remains unknown.

To investigate changes in gene expression in the retina during early-stage diabetic retinopathy, we performed differential proteomic analysis using two-dimensional electrophoresis (2-DE), in combination with matrix-assisted laser desorption ionisation time-of-flight (MALDI-TOF) mass spectrometry. The presence of αA-crystallin in pericytes was analysed by immunoblotting and immunostaining methods. Decreased amounts of αA-crystallin in human pericytes under hyperglycaemic conditions in vitro were also confirmed by immunoblotting and immunostaining. Finally, a recombinant adenovirus (Ad-*αAc-Gfp*) expressing the gene encoding αA-crystallin (*αAc*, also known as *Cryaa*) was injected into the vitreous body to examine the effect of αA-crystallin on apoptotic cell death and vessel leakage in the diabetic retina.

Methods

Animals Eight-week-old male C57BL/6 mice were obtained from KOATEC (Pyeongtaek, Korea). Mice were maintained on a standard rodent diet available, together with water, ad libitum. All experiments were approved by the Animal Care and Use Committee of Gyeongsang National University, Jinju, Korea. Diabetes was induced by intraperitoneal injection of 55 mg/kg STZ (Sigma-Aldrich, St Louis, MO, USA) in 0.05 mol/l citrate buffer (pH 4.5) on five consecutive days. Age-matched control mice received citrate buffer alone. Diabetes was defined as blood glucose levels >22.2 mmol/l 1 week after STZ injection.

Cell culture Human retinal pericytes (ACBRI 183; Cell Systems, Kirkland, WA, USA) were cultured in complete classic medium supplemented with 10% (vol./vol.) fetal bovine serum, antibiotics and human recombinant growth

factors (CultureBoost-R; Cell Systems) on attachment-factor-coated dishes. Cells were maintained in normal glucose (5 mmol/l) or high glucose (30 mmol/l) for 5 days. Mannitol was used as a control to rule out the effect of osmotic pressure.

Visualisation of retinal vasculature Retinal vasculature was assessed by angiography using high-molecular-weight-FITC-conjugated dextran (FITC-dextran, MW 2×10^6 [Sigma-Aldrich]) and tetramethylrhodamine (TMR)-conjugated dextran (TMR-dextran, MW 2×10^6 [Invitrogen, Carlsbad, CA, USA]) as previously described [25, 26]. FITC-dextran and TMR-dextran were dissolved in 0.05 mol/l sodium citrate (pH 4.5) at final concentrations of 50 mg/ml and 10 mg/ml, respectively, and infused through the left ventricle of control and diabetic mice. After FITC-dextran or TMR-dextran injection, eyes were dissected and placed in 4% (wt./vol.) paraformaldehyde (PFA) for 6 h. Flat-mounted retinas were visualised using fluorescence microscopy.

Measurement of BRB breakdown BRB breakdown was evaluated as described previously [27]. Both control and diabetic mice received injections into the left jugular vein of 45 mg/kg Evans Blue dye. At 2 h after infusion, blood was extracted through the left ventricle, and mice were perfused with PBS to completely remove the Evans Blue dye in blood vessels. Retinas were carefully dissected and the weight measured after thorough drying in a Speed-Vac (TL-100; Beckman Coulter, Fullerton, CA, USA). Next, retinas were incubated in 120 μl formamide for 18 h at 70°C to extract the Evans Blue dye, and the extract filtered through an ultra-filter (30,000 MW). Absorbance of the extract was measured with a spectrophotometer at 620 nm. The dye concentration in extracts was calculated using a standard curve of Evans Blue in formamide and normalised to the dried retinal weight.

2-DE and protein identification The total protein from each retina (50 μg/strip) was resuspended in rehydration buffer (2 mol/l thiourea, 6 mol/l urea, 4% (wt/vol.) 3-[(3-cholamidopropyl)dimethylammonio]-1-propanesulfonic acid (CHAPS), 65 mmol/l DTT, 0.5% (vol./vol.) ampholytes, 0.002% (wt/vol.) bromophenol blue), loaded onto 7 cm immobilised pH gradient (IPG) strips (Immobiline DryStrip, pH 4–11 nonlinear [Genomine, Pohang, Korea]). Isoelectric focusing was performed at 250 V for the first 15 min, followed by a gradient increase to 10,000 V for a total of 100 kVh. After isoelectric focusing and equilibration, IPG strips were subjected to 13.5% (wt/vol.) SDS-PAGE. Protein spots were visualised using silver staining according to the procedure of Kim et al [28]. Proteins were identified with peptide mass fingerprinting (PMF) analysis by Genomine using MALDI-TOF mass spectrometry (Ettan MALDI Pro; Amersham Bioscience, Piscataway, NJ, USA).

Antibodies Mouse monoclonal antibodies against αA-crystallin, α-smooth muscle actin (α-SMA), NG2 chondroitin sulphate proteoglycan (NG2) and α-tubulin were purchased from Santa Cruz Biotechnology (Santa Cruz, CA, USA), Chemicon (Tamecula, CA, USA) and Sigma-Aldrich, respectively. Rabbit polyclonal antibodies against αA-crystallin, active caspase-3 and green fluorescent protein (GFP) were obtained from Abcam (Cambridge, MA, USA) and the rabbit polyclonal PARP antibody from Cell Signaling Technology (Beverly, MA, USA). Secondary horseradish-peroxidase-conjugated anti-mouse and anti-rabbit IgG for western blotting, Alexa Fluor 350, 488 and 594 goat anti-mouse IgG, and Alexa Fluor 488 goat anti-rabbit IgG for immunofluorescent staining were purchased from Pierce Biotechnology (Rockford, IL, USA) and Invitrogen.

Immunoblotting Protein extraction and immunoblotting were performed as described previously [28]. Total protein (30 μg) was subjected to SDS-PAGE and blotted onto a nitrocellulose membrane. Blots were incubated with primary and secondary antibodies, and visualised using an enhanced chemiluminescence kit (Amersham Biosciences, Pittsburgh, PA, USA). Data were quantitatively analysed with the Soft Imaging System and SigmaGel 1.0 software (Jandel Scientific, San Rafael, CA, USA).

Immunofluorescence staining Retinal cryosections and chamber slides were incubated with blocking solution for 30 min, followed by a mixture of primary antibodies overnight with gentle rocking. After washing in PBS, sections were incubated with secondary antibodies and wet mounted using Kaiser's solution (Merck, Darmstadt, Germany). Cell apoptosis was assessed using the TUNEL assay (In situ Cell Death Detection kit [Roche, Mannheim, Germany]), as described previously [29, 30]. To determine the number of pericytes surrounding retinal vessels, angiography with infusion of TMR-dextran (Invitrogen) and immunofluorescence staining with anti-α-SMA antibody to dye vessels and pericytes were performed. All images were obtained with an IX2-DSU disk-scanning biological microscope (Olympus, Hamburg, Germany) and a confocal microscope (Axioplan 2 Imaging; Carl Zeiss, Göttingen, Germany).

RT-PCR To evaluate αA-crystallin mRNA expression in mouse retina, RT-PCR was performed. Total RNA was extracted from whole retina with TRI-reagent and RNeasy mini kit (Qiagen, Hilden, Germany), as described by the manufacturer. RNA (1 μg) was used to generate cDNA using SuperScript III reverse transcriptase (Invitrogen). *Gapdh* expression was used for normalisation. The PCR primers used in this study are listed in electronic supplementary material (ESM) Table 1.

Adenovirus injection Ad-*αAc-Gfp* was constructed using the ViraPower Adenoviral Expression system (Invitrogen), and purified with an Adeno-X Virus purification kit (Clontech Laboratories, San Jose, CA, USA), according to the manufacturer's instructions, with minor modifications. Ad-*αAc-Gfp* was deposited in the Korea Collection for Type Cultures with accession number KCTC 11844BP, as provided by the international depositary authority. Recombinant adenovirus expressing *Gfp* and αA-crystallin was injected with a 30-gauge needle into the left and right vitreous of mice, respectively, under an operating microscope. At 2 weeks after the adenovirus injection, diabetes was induced with STZ injection. The efficiency of the adenovirus infection was tested via GFP fluorescence imaging in retinal vessels.

Transmission electron microscopy Whole retinas were fixed in 2.5% (wt/vol.) glutaraldehyde solution, postfixed in 1% (wt/vol.) osmium tetroxide and dehydrated in ethanol. After embedding in Epon, thin sections were stained with 5% (wt/vol.) uranyl acetate followed by 0.4% (wt/vol.) lead citrate, and were observed with transmission electron microscopy (TEM).

Determination of adherent leucocytes Quantification of retinal leucostasis was performed as described previously [7]. After anaesthetising mice, the chest cavity was opened and the descending aorta was carefully clamped. To remove erythrocytes and non-adherent leucocytes, PBS was perfused into the left ventricle. Fixation was achieved by perfusion with 1% (wt/vol.) PFA under physiological pressure. Non-specific binding was blocked with 1% (wt/vol.) BSA in PBS, and this was followed by perfusion with TMR-isothiocyanate (TRITC)-coupled concanavalin A lectin (Vector Laboratories, Burlingame, CA, USA) to label adherent leucocytes and vascular endothelial cells. At 5 min after infusion, PBS and 1% (wt/vol.) BSA in PBS were sequentially perfused to remove residual unbound lectin. Whole retinas were carefully dissected and flat-mounted with ProLong Gold anti-fade reagent (Invitrogen). Retinas were then observed by fluorescence microscopy, and the total number of adherent leucocytes per retina determined.

Statistical analysis Data are representative of four independent values and presented as means±SEM. Data were considered significant at $p<0.05$. Statistical analyses were performed using the Kruskal–Wallis *H* test and Mann–Whitney *U* test (SPSS software).

Results

Diabetes induces vessel leakage and pericyte apoptosis in retinas Diabetic retinopathy leads to increasingly progressive alterations in the retinal vasculature. Accordingly, we evaluated the relative change in vascular permeability and pericyte apoptosis in mouse retina after 2 and 6 months of diabetes. Fluorescent angiography disclosed diabetes-induced vessel leakage in the peripheral retinas, but not in control retinas (Fig. 1a). Consistent with this finding, we observed a 1.63- and 5.86-fold increase in vessel leakage in diabetic retinas at 2 and 6 months, respectively, compared with controls, using an Evans Blue leakage assay ($p=0.047$ and $p=0.022$, respectively, Fig. 1b). Moreover, immunoblot analyses showed an increased amount of pro-apoptotic proteins such as cleaved PARP, active caspase-3 and BCL2-associated X protein (BAX; $p=0.001$, $p=0.045$ and $p=0.036$, respectively), and decreased levels of the anti-apoptotic protein B cell leukaemia/lymphoma 2 (BCL2) ($p=0.022$) in whole-retina extracts of diabetic mice (Fig. 1c). Immunofluorescence staining for TUNEL and the pericyte marker NG2 disclosed an increase in TUNEL-positive pericytes in diabetic retinas, compared with controls (Fig. 1d).

αA-Crystallin production is suppressed in diabetic retinas To investigate different protein levels in retinas 2 and 6 months after the induction of diabetes, proteomic analyses were performed using total retinal extracts. 2-DE analysis disclosed two decreased spots in diabetic retinas compared with controls (Fig. 2a). These spots were identified as the two isotypes of αA-crystallin via PMF using MALDI-TOF mass spectrometry. Immunoblot analysis further confirmed the two bands (at approximately 17 and 20 kDa) of αA-crystallin. The total amount of both αA-crystallin isoforms was decreased by 59% in diabetic retinas compared with controls ($p=0.032$, Fig. 2b). Consistent with αA-crystallin protein production, mRNA was decreased by 46% in diabetic retinas ($p=0.021$, Fig. 2c). Double immunofluorescence staining for αA-crystallin and α-SMA revealed predominant levels of αA-crystallin in retinal pericytes in both control and diabetic mice (arrows and arrowheads in Fig. 2d).

High glucose induces cell death in human retinal pericytes To identify the effect of elevated glucose levels on αA-crystallin production, human retinal pericytes (HRPs) were exposed to high glucose for 5 days. Exposure of HRPs to a high concentration of glucose (30 mmol/l; high glucose) resulted in suppression of αA-crystallin production by 76% ($p=0.027$) and enhancement of VEGF production by 1.9-fold ($p=0.014$) compared with a low concentration of glucose (5 mmol/l; normal glucose). However, high glucose did not affect the levels of pericyte markers, such as α-SMA and NG2, in HRPs (Fig. 3a). Triple immunofluorescence staining for αA-crystallin, α-SMA and TUNEL showed that αA-crystallin production decreased while TUNEL-positive cells increased in high-glucose-exposed HRPs (Fig. 3b).

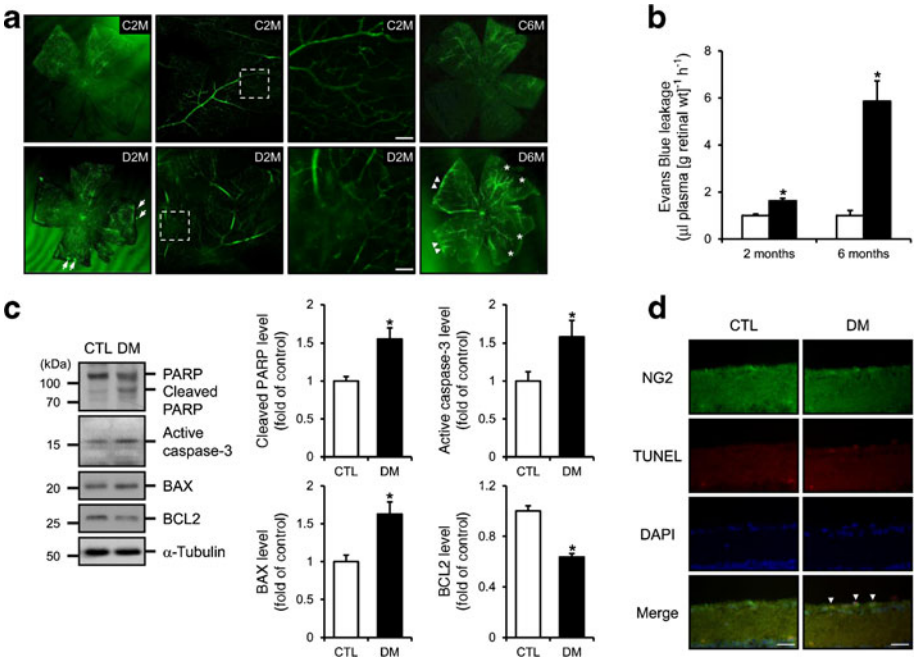

Fig. 1 Diabetes induces vascular leakage and pericyte loss in retinas. (**a**) Flat mount of retinas infused with FITC-dextran in mice 2 and 6 months after induction of diabetes and controls. Arrows show microaneurysms, arrowheads represent neovascular tufts and asterisks depict the peripheral avascular area in diabetic retinas. Scale bars, 200 μm. C2M, control 2 months; C6M, control 6 months; D2M, diabetes 2 months; D6M, diabetes 6 months. (**b**) Quantitative determination of retinal blood vessel leakage by Evans Blue dye. Data show means± SEM (n=4) (black bars, diabetes; white bars, control). (**c**) Levels of cleaved PARP, active caspase-3, BAX and BCL2 in whole-retina extracts of control and diabetic mice were determined using immunoblotting. Data are presented as means±SEM (n=4); *p<0.05 compared with control. (**d**) Double immunofluorescence staining for NG2 and TUNEL in retinal sections. Arrowheads indicate cells in the nerve fibre layer (NFL) that are α-SMA- and TUNEL-positive. Scale bars, 20 μm. CTL, control; DM, diabetes; WT, weight

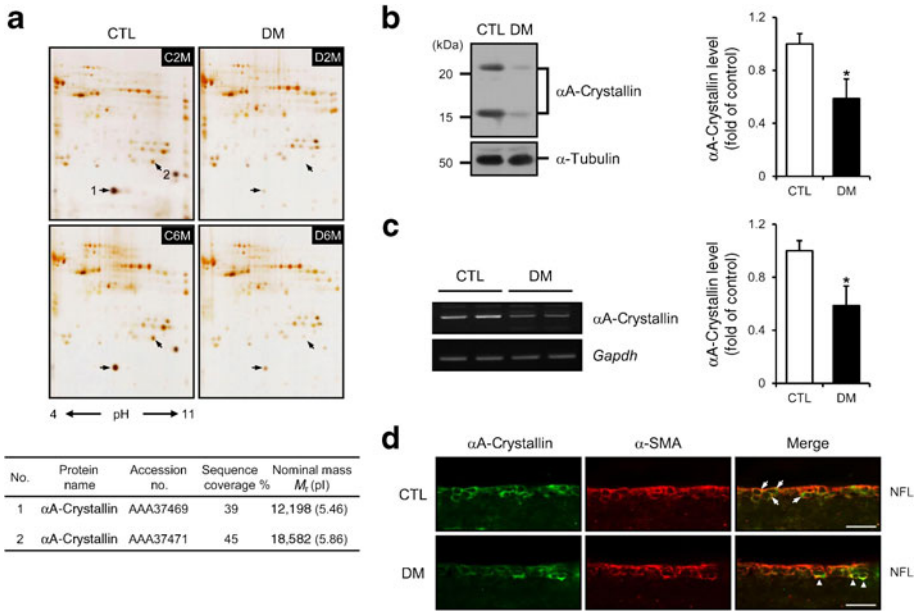

No.	Protein name	Accession no.	Sequence coverage %	Nominal mass M_r (pI)
1	αA-Crystallin	AAA37469	39	12,198 (5.46)
2	αA-Crystallin	AAA37471	45	18,582 (5.86)

Fig. 2 Diabetes decreases production of αA-crystallin in retinal pericytes. (**a**) Total retinal extract from control and 2- and 6-month-old diabetic mice were separated by 2-DE and visualised by silver staining. Two spots (arrows) in diabetic retinas were identified as αA-crystallin with MALDI-TOF and were smaller than in controls. (**b**, **c**) Protein levels and mRNA expression of αA-crystallin in control and diabetic retinas were determined via (**b**) immunoblotting and (**c**) RT-PCR. Data are presented as means±SEM (n=4); *p<0.05 compared with control. (**d**) Double immunofluorescence staining for αA-crystallin and α-SMA in retinal sections. Arrows and arrowheads indicate αA-crystallin- and α-SMA-positive cells in NFL, respectively. Scale bars, 25 μm. C2M, control 2 months; C6M, control 6 months; CTL, control; D2M, diabetes 2 months; D6M, diabetes 6 months; DM, diabetes; No., number; NFL, nerve fibre layer

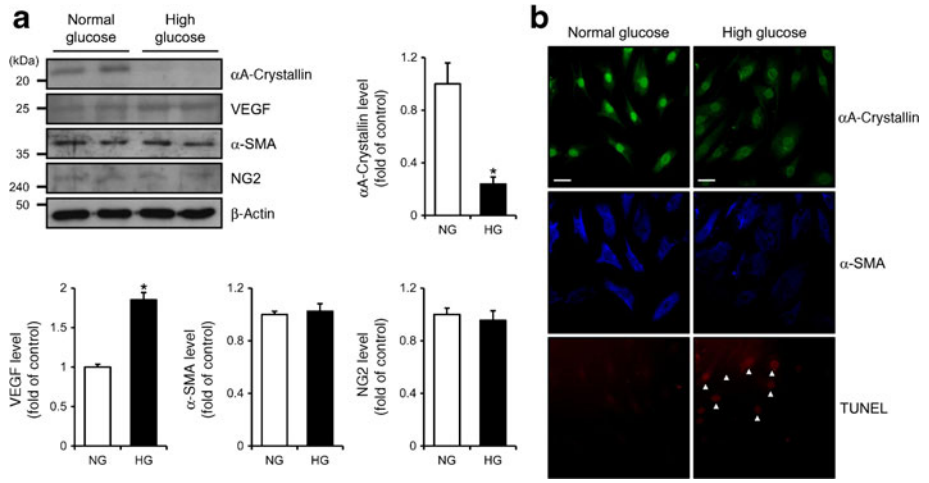

Fig. 3 Hyperglycaemia induces cell death in human retinal pericytes. (**a**) HRPs were exposed to normal (5 mmol/l) or high glucose (30 mmol/l) for 5 days. Levels of αA-crystallin, VEGF, α-SMA and NG2 were detected via immunoblotting and normalised to β-actin. Data are presented as means±SEM (n=5). *p<0.05 compared with normal glucose. (**b**) Cells were fixed on chamber slides at 5 days after glucose treatment. Triple immunofluorescence staining for αA-crystallin (green), α-SMA (blue) and TUNEL (red) was performed. TUNEL staining was used as an apoptosis marker and α-SMA staining as a pericyte marker. Arrowheads show TUNEL-positive cells in high-glucose conditions. Scale bars, 20 μm. HG, high glucose; NG, normal glucose

These results suggest that αA-crystallin production is suppressed and apoptotic cell death induced in HRPs under high-glucose conditions.

αA-Crystallin attenuates diabetes-induced retinal apoptotic cell death To verify the effects of αA-crystallin on vascular pathology in the diabetic retina, we used adenovirus-mediated gene delivery systems. Schematic diagrams of the recombinant adenovirus expressing *Gfp* and αA-crystallin-*Gfp* (Ad-*Gfp* and Ad-*αAc-Gfp*) are presented in Fig. 4a. The injection schedule for adenovirus and STZ is shown in Fig. 4b. GFP fluorescence imaging in retinal vessels showed that adenovirus-mediated GFP production continued throughout the entire 10 weeks after adenovirus injections (arrowheads in Fig. 4c). 2-DE and immunoblotting experiments confirmed the overproduction of αA-crystallin in control and diabetic retinas after the injection of Ad-*αAc-Gfp* (arrows in ESM Fig. 1a, b). Adenovirus-mediated αA-crystallin production was increased in whole-retina extracts of diabetic mice (p=0.046, Fig. 4d), but did not change in control mice. GFP production was similarly induced in all retinas after injection of recombinant adenovirus. Furthermore, levels of cleaved PARP, active caspase-3 and BAX in diabetic retina, which induce retinal cell death, were effectively reduced (p=0.003, p=0.013 and p=0.039, respectively), while BCL2 production was increased (p=0.025, Fig. 4e) with Ad-*αAc-Gfp* compared with Ad-*Gfp* treatment. These results support the theory that overproduction of αA-crystallin reduces apoptotic cell death in diabetic retinopathy.

αA-Crystallin prevents pericyte death and vascular leakage in the diabetic retina To determine whether increased production of αA-crystallin has therapeutic effects on diabetic retinopathy, the number of pericytes and retinal permeability were measured after Ad-*αAc-Gfp* treatment. TUNEL-positive retinal pericytes decreased in Ad-*αAc-Gfp*-treated diabetic mice compared with those in Ad-*Gfp*-treated diabetic mice (Fig. 5a). In parallel, angiography with TMR-dextran infusion and immunofluorescence staining for α-SMA showed that the number of retinal pericytes per vessel (0.01 mm^2) decreased after induction of diabetes compared with the control. Treatment with Ad-*αAc-Gfp* effectively blocked loss of pericytes in diabetic retinas (p=0.024, Fig. 5b). Diabetes-induced vascular leakage was significantly reduced upon Ad-*αAc-Gfp* treatment (p=0.046, Fig. 5c) In addition, TEM disclosed significantly thicker retinal capillary basement membrane in diabetic retinas compared with controls. Ad-*αAc-Gfp* attenuated pericyte loss and basement membrane thickening (Fig. 5d). TRITC-coupled, concanavalin-A-stained adherent leucocytes in vessels increased by 1.6-fold in diabetic retinas. However, Ad-*αAc-Gfp* did not significantly affect the number of adherent leucocytes compared with Ad-*Gfp* (Fig. 5e). Together, our results show that αA-crystallin is involved in diabetes-induced pericyte death and vascular leakage.

Discussion

We observed increased vessel leakage and production of pro-apoptotic proteins as well as pericyte apoptosis in mouse retina after induction of diabetes, which are characteristic features of pericyte loss and BRB breakdown [6, 7,

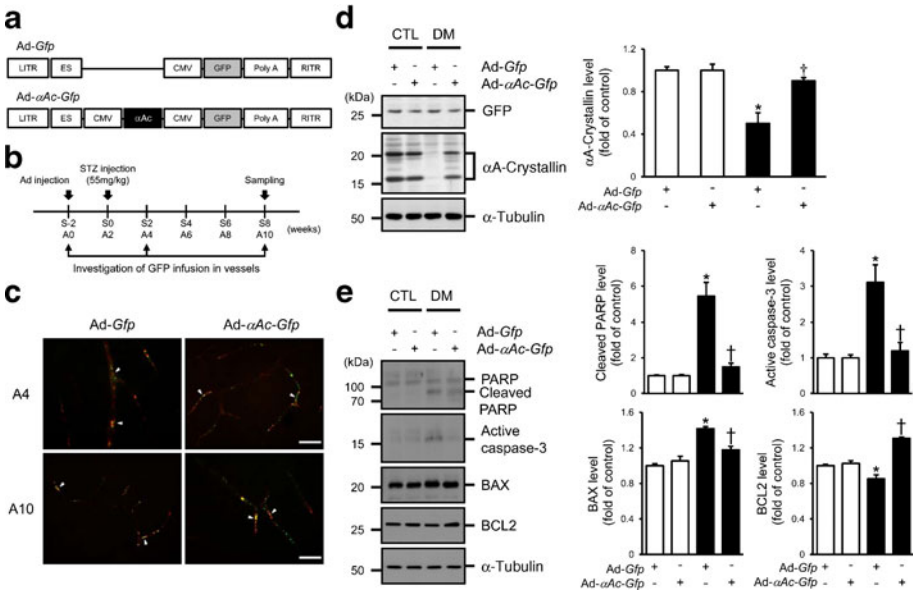

Fig. 4 Adenovirus-mediated production of αA-crystallin reduces apoptotic cell death in the diabetic retina. (**a**) Schematic diagram of adenovirus Ad-*Gfp* and Ad-*αAc-Gfp* used in this study. (**b**) Schematic diagram of the adenovirus and STZ injection strategy in the animal model. Ad-*Gfp* (1×10^9 pfu/μl, 2 μl) and Ad-*αAc-Gfp* (2×10^8 pfu/μl, 2 μl) were injected into the vitreous humour of both the control and diabetic mice. (**c**) Adenovirus-mediated gene expression was assessed by determining GFP production using fluorescence microscopy. GFP (arrowheads) was observed in retinal blood vessels at 4 and 10 weeks after adenovirus infection. Scale bars, 10 μm. (**d**, **e**) Production of αA-crystallin, cleaved PARP, active caspase-3, BAX and BCL2 in mouse retinas at 2 months from diabetes induction after adenovirus injection was detected via immunoblotting and normalised to α-tubulin production (black bars, diabetes; white bars, control). Data are presented as means±SEM (n=5). *$p<0.05$ compared with Ad-*Gfp*-treated control. †$p<0.05$ compared with Ad-*αAc-Gfp*-treated diabetic group. White bars, control; black bars, diabetes. CMV, cytomegalovirus promoter; CTL, control; DM, diabetes; ES, encapsidation signal; LITR, left inverted terminal repeats; RITR, right inverted terminal repeats

31]. Proteomic assessment of changes in gene expression confirmed decreases in two αA-crystallin subtypes in diabetic retinas compared with non-diabetic controls. Interestingly, αA-crystallin expression was specific to NG2-positive pericytes in the nerve fibre layer of both diabetic and control retinas. A previous study using gene microarrays showed that expression of many genes of the crystallin family are significantly downregulated in the retinas of mice with diabetic retinopathy. In addition, recent proteomic analysis of retina in oxygen-induced retinopathy mice showed that several crystallins, such as isoform 1 of αA-crystallin A, isoform 2 of αA-crystallin, αB-crystallin, γD-crystallin and β-A3/A1 crystallin, are downregulated [32]. Although several papers have reported that αA-crystallin is increased in the retinas of human diabetic patients and animal models of type 1 diabetes [21, 33–35], diabetes impairs the chaperone function of the α-crystallins by reducing their solubility. Increased production of αA-crystallin can protect retinal neurons from cell death through interaction with the pro-apoptotic proteins [21, 22].

Cellular apoptosis induced by hyperglycaemia occurs in many vascular cells and is crucial for the initiation of diabetic pathologies. High glucose induces pericyte apoptosis through activation of protein kinase C-δ in bovine retinal pericytes [36]. High glucose also induces mitochondrial dysfunction and apoptosis in bovine retinal pericytes. The detrimental effects of high glucose on mitochondrial function and cellular metabolism could play a role in the accelerated apoptosis associated with the retinal pericytes in diabetic retinopathy [37]. We showed, for the first time, that αA-crystallin decreased in human retinal pericytes cultured under high-glucose conditions, suggesting that decreased αA-crystallin in pericytes in response to hyperglycaemia leads to apoptotic cell death.

Advances in the field of ocular gene transfer are progressive, and viral-vector-mediated delivery of target genes that modulate endogenous protein levels in the retina may represent an effective gene therapy strategy to treat pathological angiogenesis in diabetic retinopathy [38, 39]. The viability of adenovirus as a gene therapy vector for ocular disease has recently been demonstrated in clinical trials for age-related macular degeneration and retinoblastoma [40, 41]. In the present study, we constructed a recombinant adenovirus as a vector to transfer αA-crystallin for gene therapy in diabetic retinas, and GFP fluorescence imaging showed that adenovirus-mediated gene expression was maintained in retinal vessels for up to 10 weeks after intravitreal injection. Ad-*αAc-Gfp* treatment significantly inhibited diabetes-induced αA-crystallin decrease, PARP cleavage and caspase activation. Thus, the

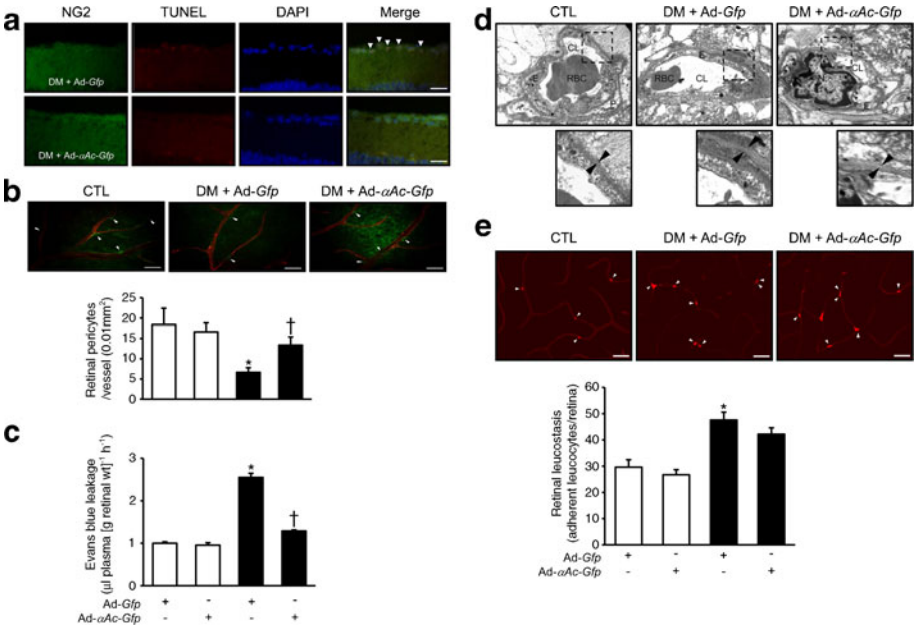

Fig. 5 Adenovirus-mediated production of αA-crystallin prevents pericyte loss and vessel leakage in the diabetic retina. (**a**) Immunofluorescence staining for αA-crystallin and TUNEL was performed in retinal sections. Arrows represent cells in the NFL that are positive for αA-crystallin and TUNEL. Scale bars, 25 μm. (**b**) Angiography with TMR-dextran infusion and immunofluorescence staining for the pericyte marker α-SMA (green) was performed. The number of pericytes per vessel (0.01 mm^2) was counted in mouse retinas 2 months after the induction of diabetes (black bars) and compared with control (white bars). Data are presented as means±SEM (n=6). (**c**) Quantitative determination of retinal blood vessel leakage by Evans Blue dye. Data are presented as means±SEM: μl plasma (g retinal dry weight)$^{-1}$ h^{-1} (n=6). (**d**) Representative transverse sections of retinal capillaries. Arrowheads, basement membrane thickness. (**e**) After in situ labelling with TRITC-coupled concanavalin A lectin, adherent leucocytes (arrowheads) were photographed at ×400 magnification. Scale bars, 50 μm. Adherent leucocytes were counted in the whole retina (black bars, diabetes; white bars, control). Data are presented as means±SEM (n=5). *p<0.05 compared with Ad-*Gfp*-treated control. †p<0.05 compared with Ad-*αAc-Gfp*-treated diabetic group. CL, capillary lumen; CTL, control; DM, diabetes; E, endothelial cell; P, pericyte; RBC, red blood cell; WT, weight

recombinant adenovirus may provide a functional approach for further studies on αA-crystallin in diabetic retina.

As pericyte loss is directly associated with vessel leakage, we examined the effect of Ad-*αAc-Gfp* on vessel leakage in diabetic retinas. TUNEL-positive pericytes were reduced in the nerve fibre layer, but the number of pericytes in retinal capillaries was increased in Ad-*αAc-Gfp*-treated diabetic mice compared with Ad-*Gfp*-treated diabetic mice. The diabetes-mediated increase in vessel leakage was effectively blocked with Ad-*αAc-Gfp* administration. These results indicate that αA-crystallin effectively inhibited pericyte loss in the retina of diabetic mice, preventing vessel leakage.

In the retinal microcirculation, comparable numbers of endothelial cells and pericytes are present in the capillary wall [42]. Pericyte loss and thickening of the basement membrane are early histopathological changes that occur in the retinal microcirculation in diabetic retinopathy [43]. Clinical evidence has shown that basement membrane thickening is directly related to hyperglycaemia and can be reduced with good diabetic control [44]. Consistent with this, our TEM findings showed pericyte loss and thickening of the basement membrane in diabetic retinas at 2 months after STZ injection that were significantly less in mice receiving Ad-*αAc-Gfp*. Although the precise mechanisms underlying basement membrane thickening are not clear, our results suggest that αA-crystallin is protective against diabetic vascular damage, including basement membrane thickening.

Increased leucocyte adhesion may induce the formation of non-perfused capillaries, which is believed to be a major contributor to the increasing capillary permeability and angiogenesis that occur with progression of diabetic retinopathy [45–47]. Indeed, we found that adherent leucocytes were significantly increased in the entire retinas 2 months after induction of diabetes compared with controls, but leucocyte adhesion was not regulated by Ad-*αAc-Gfp*. Therefore, the protective effect of αA-crystallin on pericytes is independent of leucocyte adhesion, at least in our model.

Taken together, our data indicate that increased levels of αA-crystallin effectively prevents pericyte loss and BRB breakdown in diabetic retina. Therefore, we suggest that protection of pericytes by αA-crystallin may be a potent therapeutic target for capillary abnormalities in early diabetic retinopathy.

Acknowledgements We gratefully acknowledge the experimental support of A. J. Goo, Medical Research Center for Neural Dysfunction, Gyeongsang National University, Jinju, Korea.

Funding This research was supported by the MRC programme of National Research Foundation of Korea (R13-2005-012-01001-1).

Contribution statement YHK and SYP researched data, contributed to the discussion, wrote and reviewed/edited the manuscript. JP, YSK, EMH and JYP researched data, contributed to the discussion and reviewed/edited the manuscript. GSR, HJK, SSK and GJC researched data and contributed to the discussion. WSC researched data, contributed to the discussion and reviewed/edited the manuscript. All authors approved the final version.

Duality of interest The authors declare that there is no duality of interest associated with this manuscript.

References

1. Cheung N, Mitchell P, Wong TY (2010) Diabetic retinopathy. Lancet 376:124–136
2. Nishikiori N, Osanai M, Chiba H et al (2007) Glial cell-derived cytokines attenuate the breakdown of vascular integrity in diabetic retinopathy. Diabetes 56:1333–1340
3. Skondra D, Noda K, Almulki L et al (2008) Characterization of azurocidin as a permeability factor in the retina: involvement in VEGF-induced and early diabetic blood-retinal barrier breakdown. Invest Ophthalmol Vis Sci 49:726–731
4. Orlidge A, D'Amore PA (1987) Inhibition of capillary endothelial cell growth by pericytes and smooth muscle cells. J Cell Biol 105:1455–1462
5. Yamagishi S, Kobayashi K, Yamamoto H (1993) Vascular pericytes not only regulate growth, but also preserve prostacyclin-producing ability and protect against lipid peroxide-induced injury of co-cultured endothelial cells. Biochem Biophys Res Commun 190:418–425
6. Cheung AKH, Fung MKL, Lo ACY et al (2005) Aldose reductase deficiency prevents diabetes-induced blood-retinal barrier breakdown, apoptosis, and glial reactivation in the retina of db/db mice. Diabetes 54:3119–3125
7. Joussen AM, Poulaki V, Le ML et al (2004) A central role for inflammation in the pathogenesis of diabetic retinopathy. FASEB J 18:1450–1452
8. Shen WY, Lai C, Graham C et al (2006) Long-term global retinal microvascular changes in a transgenic vascular endothelial growth factor mouse model. Diabetologia 49:1690–1701
9. Wu M, Chen Y, Wilson K et al (2008) Intraretinal leakage and oxidation of LDL in diabetic retinopathy. Invest Ophthalmol Vis Sci 49:2679–2685
10. Andley UP, Song Z, Wawrousek EF, Bassnett S (1998) The molecular chaperone alphaA-crystallin enhances lens epithelial cell growth and resistance to UVA stress. J Biol Chem 273:31252–31261
11. Welsh MJ, Gaestel M (1998) Small heat-shock protein family: function in health and disease. Ann NY Acad Sci 851:28–35
12. Andley UP (2007) Crystallins in the eye: function and pathology. Prog Retin Eye Res 26:78–98
13. Bloemendal H, de Jong WW (1991) Lens proteins and their genes. Prog Nucleic Acid Res Mol Biol 41:259–281
14. Andley UP, Song Z, Wawrousek EF, Fleming TP, Bassnett S (2000) Differential protective activity of alpha A- and alphaB-crystallin in lens epithelial cells. J Biol Chem 275:36823–36831
15. Liu B, Bhat M, Padival AK, Smith DG, Nagaraj RH (2004) Effect of dicarbonyl modification of fibronectin on retinal capillary pericytes. Invest Ophthalmol Vis Sci 45:1983–1995
16. Mao YW, Liu JP, Xiang H, Li DW (2004) Human alphaA- and alphaB-crystallins bind to Bax and Bcl-X(S) to sequester their translocation during staurosporine-induced apoptosis. Cell Death Differ 11:512–526
17. Kapphahn RJ, Ethen CM, Peters EA, Higgins L, Ferrington DA (2003) Modified alpha A crystallin in the retina: altered expression and truncation with aging. Biochemistry 42:15310–15325
18. Kapphahn RJ, Giwa BM, Berg KM et al (2006) Retinal proteins modified by 4-hydroxynonenal: identification of molecular targets. Exp Eye Res 83:165–175
19. Cherian M, Abraham EC (1995) Diabetes affects alpha-crystallin chaperone function. Biochem Biophys Res Commun 212:184–189
20. Thampi P, Zarina S, Abraham EC (2002) Alpha-crystallin chaperone function in diabetic rat and human lenses. Mol Cell Biochem 229:113–118
21. Losiewicz MK, Fort PE (2011) Diabetes impairs the neuroprotective properties of retinal alpha-crystallins. Invest Ophthalmol Vis Sci 52:5034–5042
22. Rao NA, Saraswathy S, Wu GS, Katselis GS, Wawrousek EF, Bhat S (2008) Elevated retina-specific expression of the small heat shock protein, alphaA-crystallin, is associated with photoreceptor protection in experimental uveitis. Invest Ophthalmol Vis Sci 49:1161–1171
23. Whiston EA, Sugi N, Kamradt MC et al (2008) alphaB-crystallin protects retinal tissue during *Staphylococcus aureus*-induced endophthalmitis. Infect Immun 76:1781–1790
24. Kase S, He S, Sonoda S et al (2010) alphaB-crystallin regulation of angiogenesis by modulation of VEGF. Blood 115:3398–3406
25. Kim YH, Chung IY, Choi MY et al (2007) Triamcinolone suppresses retinal vascular pathology via a potent interruption of proinflammatory signal-regulated activation of VEGF during a relative hypoxia. Neurobiol Dis 26:569–576
26. Smith LE, Wesolowski E, McLellan A et al (1994) Oxygen-induced retinopathy in the mouse. Invest Ophthalmol Vis Sci 35:101–111
27. Kim YH, Choi MY, Kim YS et al (2007) Triamcinolone acetonide protects the rat retina from STZ-induced acute inflammation and early vascular leakage. Life Sci 81:1167–1173
28. Kim YH, Choi MY, Kim YS et al (2007) Protein kinase C delta regulates anti-apoptotic alphaB-crystallin in the retina of type 2 diabetes. Neurobiol Dis 28:293–303
29. Kim YH, Kim YS, Kang SS, Cho GJ, Choi WS (2010) Resveratrol inhibits neuronal apoptosis and elevated Ca2+/calmodulin-dependent protein kinase II activity in diabetic mouse retina. Diabetes 59:1825–1835
30. Kim YH, Kim YS, Park SY, Park CH, Choi WS, Cho GJ (2011) CaMKII regulates pericyte loss in the retina of early diabetic mouse. Mol Cells 31:289–293
31. Joussen AM, Doehmen S, Le ML et al (2009) TNF-alpha mediated apoptosis plays an important role in the development of early diabetic retinopathy and long-term histopathological alterations. Mol Vis 15:1418–1428
32. Zhou L, Liu X, Koh SK, Li X, Beuerman RW (2011) Quantitative proteomic analysis of retina in oxygen-induced retinopathy mice using iTRAQ with 2D nanoLC-nanoESI-MS/MS. J Integr Omics 1:226–235
33. Kase S, Ishida S, Rao NA (2011) Increased expression of alphaA-crystallin in human diabetic eye. Int J Mol Med 28:505–511
34. Kumar PA, Haseeb A, Suryanarayana P, Ehtesham NZ, Reddy GB (2005) Elevated expression of alphaA- and alphaB-crystallins in streptozotocin-induced diabetic rat. Arch Biochem Biophys 444:77–83

35. Wang YD, Wu JD, Jiang ZL et al (2007) Comparative proteome analysis of neural retinas from type 2 diabetic rats by two-dimensional electrophoresis. Curr Eye Res 32:891–901
36. Geraldes P, Hiraoka-Yamamoto J, Matsumoto M et al (2009) Activation of PKC-[delta] and SHP-1 by hyperglycemia causes vascular cell apoptosis and diabetic retinopathy. Nat Med 15:1298–1306
37. Trudeau K, Molina AJA, Roy S (2011) High glucose induces mitochondrial morphology and metabolic changes in retinal pericytes. Invest Ophthalmol Vis Sci 52:8657–8664
38. Varda-Bloom N, Shaish A, Gonen A et al (2001) Tissue-specific gene therapy directed to tumor angiogenesis. Gene Ther 8:819–827
39. Viita H, Kinnunen K, Eriksson E et al (2009) Intravitreal adenoviral 15-lipoxygenase-1 gene transfer prevents vascular endothelial growth factor A-induced neovascularization in rabbit eyes. Hum Gene Ther 20:1679–1686
40. Campochiaro PA, Nguyen QD, Shah SM et al (2006) Adenoviral vector-delivered pigment epithelium-derived factor for neovascular age-related macular degeneration: results of a phase I clinical trial. Hum Gene Ther 17:167–176
41. Chevez-Barrios P, Chintagumpala M, Mieler W et al (2005) Response of retinoblastoma with vitreous tumor seeding to adenovirus-mediated delivery of thymidine kinase followed by ganciclovir. J Clin Oncol 23:7927–7935
42. Kuwabara T, Cogan DG (1963) Retinal vascular patterns. VI. Mural cells of the retinal capillaries. Arch Ophthalmol 69:492–502
43. Kalfa TA, Gerritsen ME, Carlson EC, Binstock AJ, Tsilibary EC (1995) Altered proliferation of retinal microvascular cells on glycated matrix. Invest Ophthalmol Vis Sci 36:2358–2367
44. Sosenko JM, Miettinen OS, Williamson JR, Gabbay KH (1984) Muscle capillary basement-membrane thickness and long-term glycemia in type I diabetes mellitus. N Engl J Med 311:694–698
45. Bursell SE, Clermont AC, Aiello LP et al (1999) High-dose vitamin E supplementation normalizes retinal blood flow and creatinine clearance in patients with type 1 diabetes. Diabetes Care 22:1245–1251
46. Kohner EM, Patel V, Rassam SM (1995) Role of blood flow and impaired autoregulation in the pathogenesis of diabetic retinopathy. Diabetes 44:603–607
47. Miyamoto K, Ogura Y (1999) Pathogenetic potential of leukocytes in diabetic retinopathy. Semin Ophthalmol 14:233–239